Nature of Atomic Bonding and Atomic Structure in the Phase-Change $Ge_2Sb_2Te_5$ Glass

M. Xu,[1,*] Y. Q. Cheng,[1] H. W. Sheng,[2] and E. Ma[1,†]

[1]*Department of Materials Science and Engineering, Johns Hopkins University, Baltimore, Maryland 21218, USA*
[2]*Department of Computational and Data Sciences, George Mason University, Fairfax, Virginia 22030, USA*

(Received 22 August 2009; published 6 November 2009)

Using electronic structure calculations, we demonstrate a global valence alternation in the amorphous $Ge_2Sb_2Te_5$, a prototype phase-change alloy for data storage. The resulting p bonding profoundly influences the local atomic structure, leading to right-angle components similar to those in the crystalline counterpart of this chalcogenide glass. The dominance of p bonding is revealed by (i) distributions of the coordination number (CN) and the bond angle, for truly bonded atoms determined based on the electron localization function, and (ii) a direct evaluation of the p (and s) orbital occupation probability for the CN = 3 Ge atoms that form 90° bonds with neighbors.

DOI: 10.1103/PhysRevLett.103.195502 PACS numbers: 61.43.Dq, 42.70.Ln, 61.43.Bn

Multicomponent chalcogenides are used as the media for high-density rewritable data storage, for optical DVDs and phase-change RAM [1]. $Ge_2Sb_2Te_5$ (GST) is a prototype alloy of these phase-change materials. A key behavior of this material for memory or storage applications is its ultrafast, reversible phase transformation (at elevated temperatures) between the amorphous GST (a-GST) and the metastable crystalline GST (c-GST) states, while exhibiting large property contrasts. This desirable feature must originate from the internal atomic structures of the two phases, as well as their unique chemical bonding features [2].

Recent theoretical and experimental efforts have led to much progress in understanding the atomic structure and bonding in GST [3]. The c-GST is now well understood as having the distorted A7 (rocksaltlike) structure with the Te atoms occupying one set of the fcc sublattice, and Ge/Sb and 20% vacancies randomly occupying the other. Resonance bonding, enabled by the existence of the long-range order of the crystalline state, has been shown to account for the physical properties of this phase [4]. In comparison, the atomic-scale structure and the chemical bonding in the a-GST is more controversial, and is likely to be of a mixed nature. Several researchers [5,6] found evidence indicating the 8-N rule, and reported [7,8] tetrahedral configuration around Ge, emphasizing the sp^3 bonding. However, recent simulations [9–12] suggest that the majority of the atoms have octahedral atomic arrangement and squarelike connections. In particular, the Ge atoms occupy the centers of octahedral as well as fourfold-coordinated positions, and a large number of the atoms have bond angles around 90°. Such ''rocksaltlike local structures'' are suggestive of p bonding, which was proposed to result from the relatively high number of average valence electrons, N_{sp}, in the alloy [7].

This Letter provides an in-depth understanding of the bonding characteristics and atomic structure in a-GST, on the level of electronic structures based on *ab initio* calculations. We identify chemically bonded atom pairs via electron localization function (ELF) analysis, in lieu of the ambiguous distance cutoff method commonly used in previous work. This allows a reliable account of the coordination numbers (CNs) and the bond angles, for an atom with its neighbors. The prominent p bonding is also demonstrated by the occupation probabilities for the s and p orbitals, and explained from the perspective of each of the three constituent elements that undergo valence alternation [13] upon alloying.

Our *ab initio* molecular dynamics simulations were carried out using the Vienna *ab initio* simulation package (VASP) [14], with canonical (NVT) ensembles. The temperature was controlled using the Nose thermostat [15]. Projector augmented plane waves (PAW) [16,17] with the Perdew-Wang exchange-correlation potentials have been adopted [18]. The simulation is performed on the Γ point only. Periodic boxes having the rocksalt structure and fixed atomic ratios (Ge:Sb:Te:vacancies = 2:2:5:1) were melted at 3000 K for 3000 time steps (9 ps) and quenched to room temperature at the rate of 20 K/ps, followed by relaxation for 3000 time steps. The last 1000 configurations were used to calculate the structural parameters. By comparing results for different box sizes (63, 126, and 189 atoms), we conclude that the results are independent of the size of the system. An example of the quenched glass structure is shown in the inset of Fig. 1(a).

The total and partial pair-correlation functions (PCFs) are calculated from the atomic positions and depicted in Fig. 1(a), together with the bond-angle distribution in Fig. 1(b). The total PCF shows three peaks: the first peak is located around 2.87 Å, corresponding to the distance of the nearest-neighbors in a-GST. It is found that the first-neighbor pairs are mainly composed of Ge-Te (peak at 2.78 Å) and Sb-Te (peak at 2.92 Å), with very few Ge-Ge, Sb-Sb, Ge-Sb, and Te-Te. This is consistent with previous experimental findings [19]. The Te-Te pairs, on the other hand, are the main contributor to the second peak

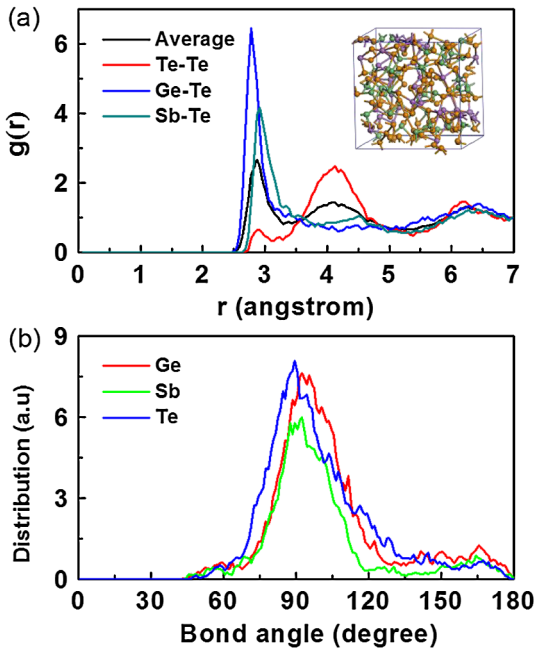

FIG. 1 (color online). Calculated (a) total and partial pair-correlation functions and (b) bond-angle distributions of a-GST. Inset in (a) displays a ball-stick model (189 atoms) of the a-GST, quenched from liquid to 300 K. The density is 6.11 g/cm^3. The green (medium gray), purple (dark gray), and yellow (light gray) balls represent Ge, Sb, and Te atoms, respectively.

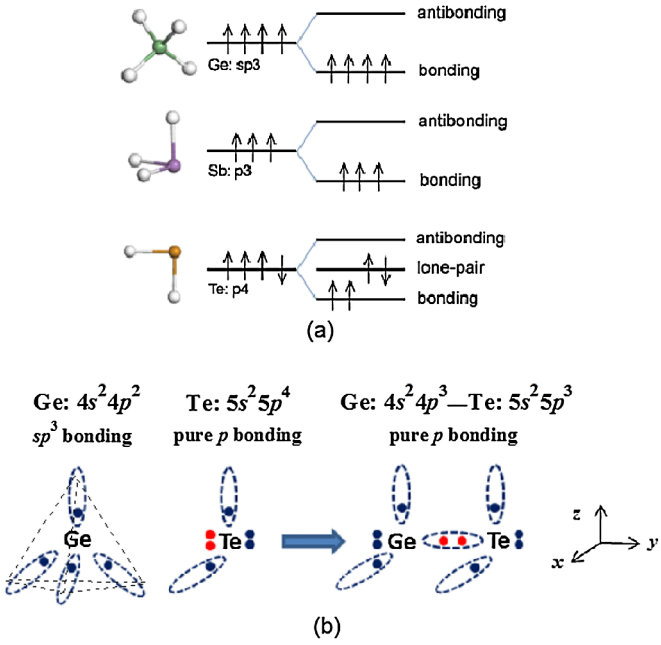

FIG. 2 (color online). Schematic of (a) the electronic structure and the bonding geometry of Ge, Sb, and Te in an *ideal* glass model, and (b) the valence alternation process between Ge and Te. In 3D space, the sp^3 bonds have the tetrahedral shape with bond angles of 109°, while the p bonds are perpendicular to each other. The valence alternation changes not only the CN of the Ge and Te, but also the bond angle around Ge.

in the total PCF, at a distance of $\sim\sqrt{2}L$, where L is the bond length of Te-Ge or Sb-Te. Noting that the bond-angle distribution has its peak around 90° in Fig. 1(b), one can envision that the structure contains a large number of Te-Ge(Sb)-Te components: the Te-Ge(Sb)-Te forms a right-angle bond such that the distance between Te-Te is $\sim\sqrt{2}L$. Here as a first-cut qualitative treatment, the bonded atoms in Fig. 1(b) were determined using a nearest-neighbor cutoff distance of 3.2 Å [20]. A more rigorous method will be proposed below for the quantitative analysis.

In an "ideal" covalent glass model [21], each constituent atom [Ge, Sb, and Te, as shown in Fig. 2(a)] strives to obey the "8-N rule": CN = 8-N [21,22] where N is the number of the valence electrons. For Ge, its four valence electrons, $4s^24p^2$, hybridize into four sp^3 orbitals to lower the total energy, thus forming the 109°-angle tetrahedral bonding typical of the IVB group solids. The Sb atom has two 5s electrons which are usually not involved in covalent bonding, and the remaining three 5p electrons occupy the three p orbitals. The Te atom has one more electron than Sb, such that one of the p orbitals is fully occupied by two paired electrons, which are called nonbonding or "lone-pair" electrons, leaving two bonding valence electrons [23]. The bonds of Sb and Te tend to have the 90° right angle because the p orbitals are perpendicular to one another.

As seen in the bond-angle distribution shown in Fig. 1(b), the Sb and Te in the a-GST have predominantly right-angle bonds, much like in the ideal models above, and resembles the scenario in c-GST (rocksaltlike structure) to a large extent. However, interestingly most of the Ge atoms also have bond angles close to 90°, but not 109°. This difference results from the changes in the electronic structure when Ge interacts with Te in GST, in a process known as *valence alternation* [13]. This scenario is schematically illustrated in Fig. 2(b). The two lone-pair electrons of Te [red (light gray) dots in Fig. 2(b)] are in a higher-energy state compared to the bonding electrons, so Te tends to donate one of them to the neighboring Ge, and becomes trivalent as a result. In the meantime, the sp^3 hybridization in Ge is replaced by p bonding via the three p orbitals, see Fig. 2(b). In this process, there is an energy cost when the four sp^3 electrons break into two s electrons and two bonding p electrons, because the stability resulting from the hybridization is lost. However, the energy decreases when the two energetic lone-pair electrons convert to bonding p electrons. The overall energy change of the entire system is presumably composition dependent, and for Ge atoms the sp^3 hybridization and local tetrahedral configuration are more likely to be converted into p bonding in a Te-rich environment, where the energetic lone-pair p electrons are abundant [7]. As a result of the valence

alternation, both of Ge and Te atoms become threefold coordinated with the p bonds. The bond angles around Ge tend to become 90°, as illustrated in Fig. 2(b).

There are two challenges to confirm the dominant role of the threefold 90° p bonds. The first is that we need to identify the neighbors that are truly bonded with the center atom (excluding the weakly bonded atoms that happen to be within the distance cutoff), such that the true CN and hence bond angles can be reliably determined. To this end, we adopt a new method to calculate the number of chemically bonded neighbors for each atom. The primary signature of a covalent bond is the sharing and localization of valence electrons between the bonding atoms. The degree of localization and hence the relative strength of a covalent bond can be reflected by the electron localization function [24,25],

$$\mathrm{ELF} = \frac{1}{1 + (D_\sigma / D_\sigma^0)^2} \tag{1}$$

where D_σ is a measure of Pauli repulsion and scales with the probability density of finding another same-spin electron near the reference electron. The smaller this probability, the more localized is the latter electron [25]. D_σ^0, which is used to normalize D_σ, is the D_σ value in a homogeneous electron gas having the same local spin-density. ELF = 0.5 thus represents the same level of Pauli repulsion as in the homogeneous electron gas, and a higher ELF value indicates that the electrons are more localized (ELF = 1 can be interpreted as perfect localization).

VASP quantifies the ELF values [26,27] on a 60 × 60 × 60 grid in the cubic box. To obtain the ELF profile from one atom to a neighboring atom, we first connect them with a tube (radius = 0.36 Å), which is evenly divided into 21 sections. ELF data points included in each section are then averaged, and the 21 averaged ELF values profile the bond between the two atoms (the minimum in the middle reflects the relative bond strength). Examples are shown in Fig. 3(a), for a particular Ge atom and its neighbors. This ELF approach is more physical than merely relying on interatomic distances: although it is generally true that closer neighbors are more likely to be actually bonded, many exceptions exist, especially for those atoms around the cutoff distance in our system. Overlaying the ELF profiles of all atom pairs in Fig. 3(b), we observe an obvious upper band, consisting of atom pairs with relatively high degree of localization and hence higher bond strength. Using the ELF threshold of 0.58 to eliminate the poorly bonded pairs, the truly bonded pairs are identified and used for further analysis to determine the CN and bond-angle distribution. The CN of Ge (and Te) obtained as such, Fig. 3(c), obviously deviates from 4 (and 2) in the ideal glass model, and nearly 70% of Ge and 40% of Te are triply bonded (since the overall composition is Te-rich, the majority of Te remains twofold bonded). Moreover, the threefold Ge atoms (CN = 3) have bond angles around

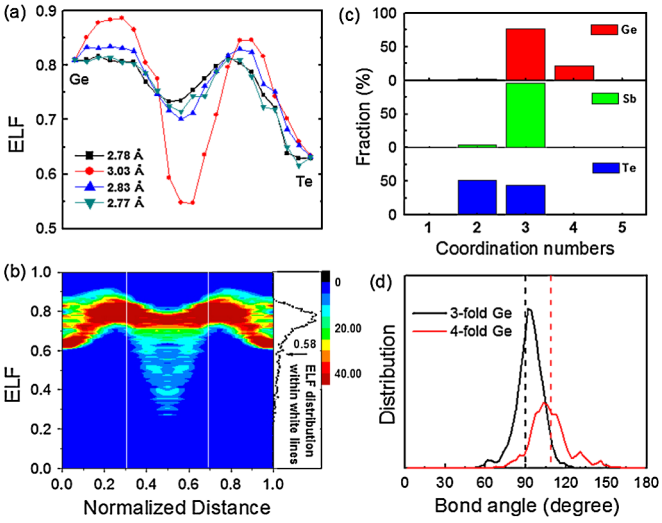

FIG. 3 (color online). (a) Representative ELF profiles for a Ge atom and its neighbors (the neighboring atom at 3.03 Å appears to be not covalently bonded). (b) The ELF distribution between all atom pairs within a distance cutoff of 3.5 Å. The threshold ELF value (0.58 for actual bonding) is labeled by the arrow, which cuts across the valley separating the peak and tail. (c) The CN around each element, for chemically bonded neighbors. (d) Bond-angle distributions for Ge atoms with CN = 3 and CN = 4, respectively. The 90° and 109° angles are marked with dashed lines.

90°, Fig. 3(d), while the fourfold ones (CN = 4) show a peak at 109°. Figures 3(c) and 3(d) are strong indications of preferred p bonding away from sp^3, as a result of the valence alternation in a-GST. A qualitative comparison shows that the projected electron density of states (DOS)

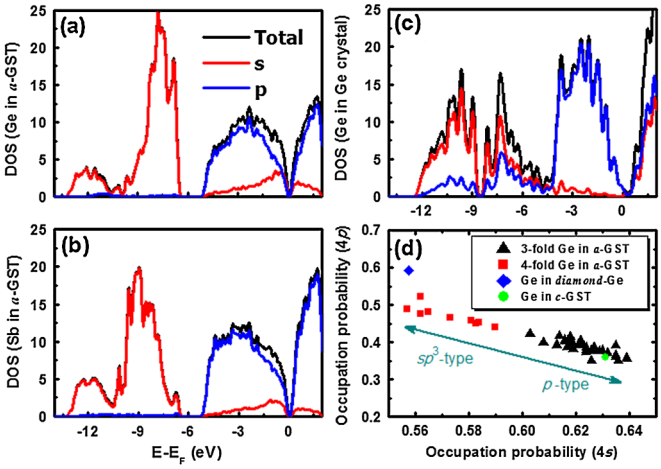

FIG. 4 (color online). The total and projected DOS for (a) Ge in a-GST, (b) Sb in a-GST, and (c) Ge in diamond Ge. (d) Occupation probability of 4s and 4p orbitals (within the core region) for Ge atoms in a-GST, showing that the CN = 3 and CN = 4 Ge atoms belong to two bifurcated groups. Average values for Ge in crystalline Ge (sp^3) and Ge in c-GST (p-type bonding in rocksalt structure) are also given as references.

of Ge in *a*-GST, Fig. 4(a), is in fact similar to that of the *p*-bonded Sb, Fig. 4(b), but very different from the known sp^3 bonding in diamond Ge [Fig. 4(c)].

The next challenging task is to unequivocally confirm that the ~90° bonds of the threefold Ge atoms are indeed of the *p* type as expected, whereas the fourfold Ge atoms possess sp^3-type bonding. To uncover the difference between these two groups, we assess the VASP-evaluated relative occupation of the 4*s* and 4*p* orbitals, obtained by integrating the site- and orbital-projected DOS within the core region (i.e. within the Wigner-Seitz radius of 1.217 Å) for each Ge atom. For sp^3 bonding, 4*s* electrons are more involved in the chemical bond between atoms via sp^3 hybridization, while for pure *p* bonding, 4*s* electrons are relatively low lying in their parent atoms. In view of this, for Ge atoms with sp^3-like bonding, the occupation probability of 4*s* orbital within the core region is expected to be lower, as more of them are outside the core in the valence region, actively participating in bonding. For *p* bonded Ge, in comparison, the occupation probability in the core region is higher for 4*s* orbitals, and lower for 4*p* orbitals as the outside valence region is dominated by the *p* electrons. The above scenario is indeed observed in our *a*-GST [Fig. 4(d)]. The CN = 3 Ge atoms show high 4*s* and low 4*p* occupation in the core, indicating *p* bonding and bifurcating themselves from the fourfold Ge atoms, which all have relatively low 4*s* occupation in the core region, demonstrating sp^3-like character. The overall trend (arrows) is also in line with the behavior of the two contrasting references, diamond Ge (sp^3 bonding) and Ge in *c*-GST (*p* bonding).

In summary, *ab initio* molecular dynamics simulations reveal that the *a*-GST is characterized by rocksaltlike, ''right-angled'' local atomic motifs. This atomic structure originates from the valence alternation between Ge and Te, which destabilizes the sp^3 hybridization and promotes *p* bonding among all the constituent species. As a result, the CNs of Ge and Te both shift towards 3, and the bond angles around Ge become dominated by ~90°. There is some indication of a mixed behavior: some Ge atoms may retain the sp^3 character with CN = 4 and tetrahedral-like configuration. The new method of basing the analysis on chemically bonded pairs determined using ELF may be useful for studying other phenomena in *a*-GST and more complex phase-change materials. The atomic bonding and atomic structure uncovered here for *a*-GST, especially the connections with those in *c*-GST, are expected to have implications for understanding its crystallization behavior.

This work was supported by U.S.-DOE-BES, Division of Materials Sciences and Engineering, under Contract No. DE-FG02-09ER46056.

*mx@jhu.edu
†ema@jhu.edu

[1] W. Welnic and M. Wuttig, Mater. Today **11**, 20 (2008).
[2] S. R. Ovshinsky, Phys. Rev. Lett. **21**, 1450 (1968).
[3] M. Wuttig and N. Yamada, Nature Mater. **6**, 824 (2007).
[4] K. Shportko, S. Kremers, M. Woda, D. Lencer, J. Robertson, and M. Wuttig, Nature Mater. **7**, 653 (2008).
[5] D. Lencer, M. Salinga, B. Grabowski, T. Hickel, J. Neugebauer, and M. Wuttig, Nature Mater. **7**, 972 (2008).
[6] W. Welnic, S. Botti, L. Reining, and M. Wuttig, Phys. Rev. Lett. **98**, 236403 (2007).
[7] C. Steimer, V. Coulet, W. Welnic, H. Dieker, R. Detemple, C. Bichara, B. Beuneu, J. P. Gaspard, and M. Wuttig, Adv. Mater. **20**, 4535 (2008).
[8] A. V. Kolobov, P. Fons, A. I. Frenkel, A. L. Ankudinov, J. Tominaga, and T. Uruga, Nature Mater. **3**, 703 (2004).
[9] S. Caravati, M. Bernasconi, T. D. Kuhne, M. Krack, and M. Parrinello, Appl. Phys. Lett. **91**, 171906 (2007).
[10] Z. M. Sun, J. Zhou, A. Blomqvist, B. Johansson, and R. Ahuja, Phys. Rev. Lett. **102**, 075504 (2009).
[11] J. Hegedus and S. R. Elliott, Nature Mater. **7**, 399 (2008).
[12] J. Akola and R. O. Jones, Phys. Rev. B **76**, 235201 (2007).
[13] M. Kastner, D. Adler, and H. Fritzsche, Phys. Rev. Lett. **37**, 1504 (1976).
[14] G. Kresse and J. Furthmuller, Comput. Mater. Sci. **6**, 15 (1996).
[15] M. P. Allen and D. J. Tidesley, *Computer Simulation of Liquids* (Clarendon, Oxford, 1989).
[16] P. E. Blochl, Phys. Rev. B **50**, 17953 (1994).
[17] G. Kresse and D. Joubert, Phys. Rev. B **59**, 1758 (1999).
[18] Y. Wang and J. P. Perdew, Phys. Rev. B **44**, 13298 (1991).
[19] S. Kohara, K. Kato, S. Kimura, H. Tanaka, T. Usuki, K. Suzuya, H. Tanaka, Y. Moritomo, T. Matsunaga, N. Yamada, Y. Tanaka, H. Suematsu, and M. Takata, Appl. Phys. Lett. **89**, 201910 (2006).
[20] Z. M. Sun, J. Zhou, A. Blomqvist, B. Johansson, and R. Ahuja, Appl. Phys. Lett. **93**, 061913 (2008).
[21] N. F. Mott, Philos. Mag. **19**, 835 (1969).
[22] N. F. Mott, Adv. Phys. **16**, 49 (1967).
[23] R. Zallen, *The Physics of Amorphous Solids* (Wiley Classics Library Edition, New York, 1998).
[24] B. Silvi and A. Savin, Nature (London) **371**, 683 (1994).
[25] A. D. Becke and K. E. Edgecombe, J. Chem. Phys. **92**, 5397 (1990).
[26] S. Andreas, J. Ove, F. Jurgen, A. Ole Krogh, P. Heinzwerner, and S. Hans Georg von, Angew. Chem., Int. Ed. Engl. **31**, 187 (1992).
[27] G. V. Gibbs, D. F. Cox, N. L. Ross, T. D. Crawford, J. B. Burt, and K. M. Rosso, Phys. Chem. Miner. **32**, 208 (2005).